24th COBEM - 2017

24th ABCM International Congress of Mechanical Engineering
December 3-8, 2017, Curitiba, PR, Brazil

COBEM-2017-1210
$\mathcal{H}_\infty$ AND MODEL REFERENCE REFERENCE ADAPTIVE CONTROL OF A SERIES ELASTIC ACTUATOR FOR ROBOTIC REHABILITATION: PRELIMINARY RESULTS

Jonathan C. Jaimes
Juan Carlos Perez-Ibarra
Felix Mauricio Escalante
Andres L. Jutinico
Marco H. Terra
Adriano A. G. Siqueira
University of São Paulo, São Carlos School of Engineering
Av. Trabalhador São-Carlense, 400, São Carlos-SP, 13566-590, Brazil
jonathancj@usp.br, jcperezibarra@sc.usp.br, ajutinico@usp.br, maurinho707@usp.br, terra@sel.eesc.usp.br, siqueira@sc.usp.br

Abstract. *Impedance Control of Series Elastic Actuators (SEAs) has been an established solution to dose the amount of assistance during robotic therapy. However, this approach requires an internal force control loop whose performance is sensitive to variations of the human dynamics. In previous papers we conclude that for this configuration, only a variable-gain scheme that modify the force control parameters according to the human activity can ensure high performance for all of those variations. In this paper, we propose an adaptive control strategy based on $\mathcal{H}_\infty$-synthesis and Model Reference Adaptive Control (MRAC). We use an $\mathcal{H}_\infty$ force controller previously synthesized for an SEA-based robotic platform for ankle rehabilitation. The control signal provided by the $\mathcal{H}_\infty$ controller guarantee robust stability and high performance of the platform's force controller during a reference condition. For the remaining conditions, a MRAC adjusts the control signal by estimating adequate control parameters for the actual plant, compensating the variations of the system dynamics from the reference model. Results from simulations for four different conditions of operation shown improvements of the force tracking performance using the proposed adaptive scheme. This research is a starting point for future implementation in the actual platform and others SEA-based robotic systems.*

Keywords: *Force Control, Series Elastic Actuators, $\mathcal{H}_\infty$ Control, Model Reference Adaptive Control*

1. INTRODUCTION

In recent years, several robotic devices have been developed to improve rehabilitation strategies of people with locomotor disorders (Chang and Kim, 2013; Maciejasz *et al.*, 2014). In Goncalves *et al.* (2014), our laboratory presented the development and evaluation of an impedance-controlled robotic platform for ankle rehabilitation. This platform is an 1-DOF robotic system actuated by a series-elastic actuator (Pratt and Williamson, 1995). Also, the platform is impedance-controlled (Hogan, 1985) to ensure safe force levels while it assists the human movements during therapy. Impedance control of the platform requires an explicit inner force control loop whose performance is sensitive to uncertainties and time-varying arising from human-robot interaction. In Perez-Ibarra *et al.* (2017) we analyze how variations of the human impedance had effects on the performance of the SEA's force controller. We conclude that a fixed-gain controller can not guarantee stability and high performance of the human-robot system for all the possible variations of the human dynamics, since an specific controller designed to have high performance for an given human behavior (p.e., being resistive) does not have the same performance during other behaviors (p.e., being passive). Our hypothesis is that a variable-gain scheme that modify the control parameters according to the human activity should maintain high performance of the force control during the complete human-robot interaction.

In Jutinico *et al.* (2017a,b), we designed a force controller using a Robust Markovian approach considering three "operation modes" of the system, namely fixed, human resistive and human passive. By using this apporach, we achieve robust stability and improve the performance for all the operation modes. Adaptive control theory has been used in human-robot interaction settings to deal with variations of the human dynamics. For instance, in Sharifi *et al.* (2014) is presented a combination between Impedance Control and Model Reference Adaptive Control (MRAC) to control a 5-DOF robotic manipulator. They use the parameters of a stable reference impedance model and makes the closed-loop dynamics of the robot similar to that of the reference model. Adaptive configurations also have been used for rehabilitation purposes.

Wolbrecht *et al.* (2008) used a standard model-based adaptive control approach for a pneumatic-based orthosis for post-stroke upper limbs training. Hussain *et al.* (2013) introduced an adaptive impedance control scheme for a pneumatic-based robotic device for gait training of neurologically impaired subjects. Regarding the control of SEA-based devices for human-robot interaction, Calanca and Fiorini (2014) proposed two force control adaptive algorithms based on a reference model and considering the human joint as a simplified second order model with stiffness, damping and inertia. Finally, in (Lopez *et al.*, 2014) was designed an SEA-based exoskeleton for lower limb training. Their results implementing an adaptive control law showed that the robot was able to adapt to different users without the adjustment of the controller gain when the user is changed.

In this paper, we present preliminary simulation results with the purpose to understand how the adaptation of the platform's controller parameters according to the variation of the human impedance can improve the force control performance. As starting point we use the $\mathcal{H}_\infty$ force control synthesized for the platform in Perez-Ibarra *et al.* (2017). This controller guaranteed robust stability although the variation of the human dynamics. Since the performance was related to the output mechanical impedance of the load, we obtained the best performance when the platform is mechanically fixed and the worst when the platform is completely free to move. We propose to use the control signal provided by the $\mathcal{H}_\infty$ controller, which was synthesized for the "fixed" case. Then, define this condition as the reference model, and use a MRAC to compensate the variations of the system dynamics from that model.

This paper is organized as follows: Section 2 introduces the SEA-based robotic platform and its respective dynamic model; Section 3 describes the design of the controllers; Section 4 reports experimental results; finally, Section 5 provides the conclusions and some final remarks for future works.

2. SYSTEM DESCRIPTION AND MODELLING

The SRPAR (Fig.1a) is a robotic platform that uses a DC motor fixed to a ballscrew through a belt and pulleys. A recirculating ballscrew nut converts the rotational motion of the worm screw into linear motion. When the motor is driven, the nut moves a support piece forward or backward, compressing a pair of steel springs. The springs move a kinematic chain that converts linear force in torque and transmit it to the user. Complete descriptions and mathematical models of the SRPAR dynamics are presented in Perez-Ibarra *et al.* (2017) and Jutinico *et al.* (2017a,b).

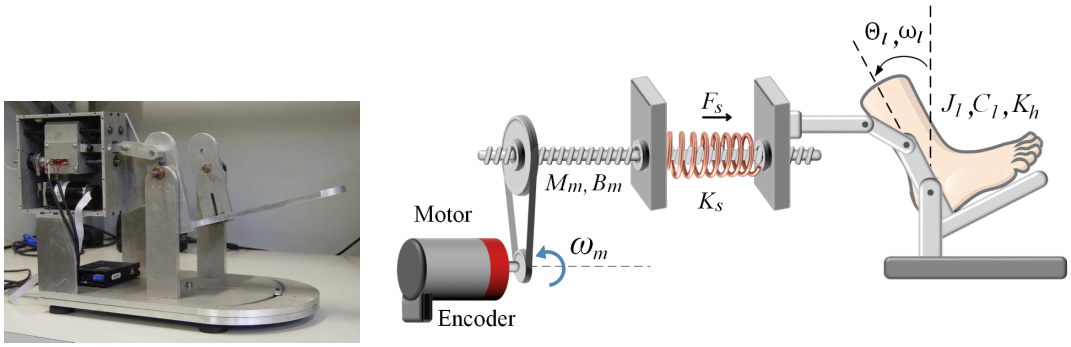

(a) Physical device. (b) Squematic Model.

Figure 1. SRPAR: SEA-based platform for ankle robotic rehabilitation. (Goncalves *et al.*, 2014).

Consider the transfer function, G_p (s), between the spring force, $y_p = F_s$, and the desired motor velocity, $u_p = \omega_m^d$, as following,

$$G_p(s) = \frac{F_s}{\omega_m^d} = \frac{\rho N K_{PI} K_s K_t Z_l}{\bar{Z}_m K_{PI} Z_l s + K_s \left(Z_l + \bar{Z}_m K_{PI}\right)}, \tag{1}$$

where ρ is a rotational-to-linear factor, N is the pulley ratio, $K_{PI} = K_p + \frac{K_i}{s}$ corresponds to the inner velocity control with proportional and integral gains K_p and K_i respectively, K_s is the spring constant and K_t is the motor constant.

In Eq. (1), $\bar{Z}_m = Z_m/K_{PI} + (\rho N)^2 K_t$, where $Z_m = M_m s + B_m$, is the mechanical impedance of the motor-transmission system with M_m and B_m as the equivalent mass and damping for the motor transmission. In addition, $Z_l = \mathcal{J}^{-2}\left(J_l s + C_l + K_h/s\right)$ is the mechanical impedance of the human-load system, where $\mathcal{J}$ is the Jacobian that maps linear and angular forces, $J_l = J_{plat} + J_h$ and $C_l = C_{plat} + C_h$ are respectively the combined inertia and damping for human and platform, and K_h is the human stiffness. Subscripts $_{plat}$ and $_h$ stand for platform and human, respectively.

The transfer function $G_p(s)$ is expressed in the form

$$G_p(s) = k_p \frac{N_p(s)}{D_p(s)} = k_p \cdot \frac{s^3 + b_{2,p}s^2 + b_{1,p}s + b_{0,p}}{s^5 + a_{4,p}s^4 + a_{3,p}s^3 + a_{2,p}s^2 + a_{1,p}s + a_{0,p}}, \tag{2}$$

Consider as reference model the condition with best performance in Perez-Ibarra *et al.* (2017), i.e. when $Z_l \to \infty$,

$$G_p(s)|_{Z_l \to \infty} = \frac{\rho N K_s K_t K_{PI}}{\bar{Z}_m K_{PI} s + K_s}. \tag{3}$$

The transfer function of the reference model, $W_m(s)$, is obtained by replacing the parameter values from Table 1 in Eq. (3), by

$$W_m(s) = k_m \frac{N_m(s)}{D_m(s)} = \frac{k_m(s + b_{0,m})}{s^3 + a_{2,m}s^2 + a_{1,m}s + a_{0,m}} = \frac{3.8 \cdot 10^4(s + 40.5)}{s^3 + 786.6s^2 + 2.5 \cdot 10^{10}s}. \tag{4}$$

Table 1. Platform Parameters

Parameter	Value	Parameter	Value	Parameter	Value	Parameter	Value
N	2	K_t (N·m/A)	0.0302	C_{plat} (N·m·s/rad)	3.5	K_s (N/m)	320000
ρ	800π	B_m (N·m·s)	72573	J_{plat} (kg· m^2)	0.0013	K_p (A·s/rad)	30.42
		M_m (kg)	383.42	$\mathcal{J}$ (m/rad)	0.03	K_i (A/rad)	1.23

3. CONTROLLER DESIGN

3.1 Impedance Control

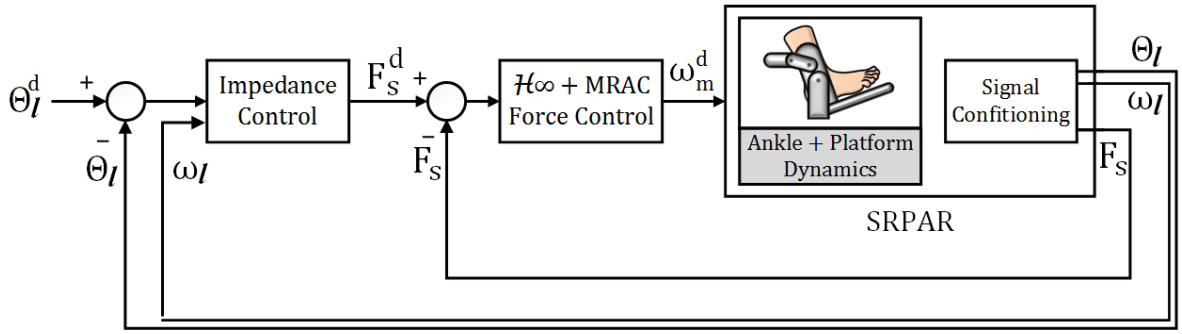

Figure 2. Impedance- and Force Control of the SRPAR.

Figure 2 shows the overall control architecture of the SRPAR device. Using a cascade configuration, the output of the impedance control block is the reference for the force control block. The impedance control establishes a relation between the actuator force and the desired angular trajectory of the load. This relation is the mechanical impedance yielded by the actuator respect to the load motion and is given by

$$F_s^d = \mathcal{J}^{-1}\tau_r = \mathcal{J}^{-1}\left(K_v(\Theta_l^d - \Theta_l) + B_v\,\omega_l\right), \tag{5}$$

where τ_r is the platform torque, K_v and B_v are respectively the virtual stiffness and damping of the controller, Θ_l, Θ_l^d and ω_l are the angular position, desired position and angular velocity of the load respectively. Both the angular trajectory and virtual parameters are mapped by the Jacobian $\mathcal{J}$.

3.2 $\mathcal{H}_\infty$ and MRAC Force Control

A model reference adaptive control (MRAC) is projected to use the output of the $\mathcal{H}_\infty$ force control block and to make the closed-loop dynamics of the system similar to the reference model. (Figure 3)

The $\mathcal{H}_\infty$ force control was computed in Perez-Ibarra *et al.* (2017), and is given by,

$$K_c(s) = \frac{2.78\text{e}9s^3 + 2.18\text{e}12s^2 + 6.95\text{e}13s + 6.95\text{e}10}{s^4 + 5.52\text{e}6s^3 + 3.34\text{e}11s^2 + 1.35\text{e}13s + 4.3\text{e}6}. \tag{6}$$

The adaptive control methodology described in this section is based in the Direct MRAC scheme for SISO plants proposed in Ioannou and Sun (2013), Figure 4. The MRAC objective is to determine the plant input, u_p, so that the closed-loop transfer function $G_c(s)$ between the plant response, y_p, and the reference, r, has stable poles and is equal to a transfer function of the reference model $W_m(s)$. Such a transfer function matching guarantees that for any reference input signal $r(t)$, the plant output y_p converges to y_m exponentially fast.

To obtain an implementable control law, $G_p(s)$ and $W_m(s)$ must satisfy the following assumptions:

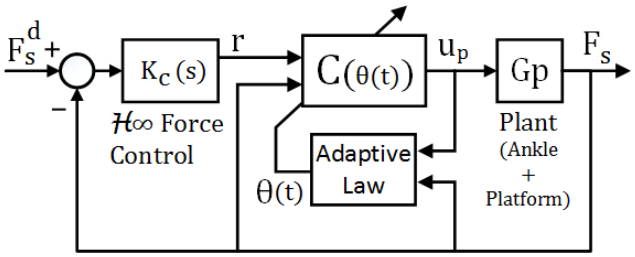

Figure 3. Proposed MRAC and $\mathcal{H}_\infty$ Force control.

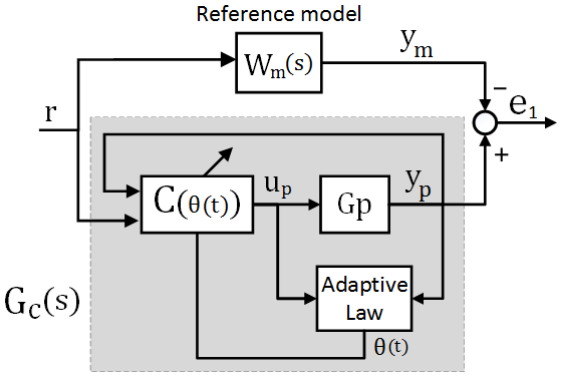

Figure 4. Direct MRAC scheme.

- $N_p(s)$ is a monic Hurwitz polynomial of degree m_p,
- $D_p(s)$ is a monic polynomial of degree $n_p \leq n$,
- the sign of k_p and the relative degree $n^* = n_p - m_p$ of $G_p(s)$ are known,
- $N_m(s)$ and $D_m(s)$ are monic Hurwitz polynomials of degree q_m, p_m respectively, where $p_m \leq n$, and
- the relative degree $n_m^* = p_m - q_m$ of $W_m(s)$ is the same as that of $G_p(s)$.

The control law acting on the plant, u_p, is shown in Figure 5 and is given by:

$$u_p = \theta_1^T(t) \cdot \frac{\alpha(s)}{\Lambda(s)} u_p + \theta_2^T(t) \cdot \frac{\alpha(s)}{\Lambda(s)} F_s + \theta_3(t) \cdot F_s + c_0(t) \cdot r, \tag{7}$$

where $\theta_1, \theta_2, \theta_3, c_0$ are the controller parameters to be computed by the adaptive law, $\alpha(s) = [s^3, s^2, s, 1]^T$, and $\Lambda(s)$ is an arbitrary monic Hurwitz polynomial of degree $n-1$ that contains $N_m(s)$ as a factor by

$$\Lambda(s) = \Lambda_0(s) N_m(s) = \Lambda(s) = (s + \frac{k_p}{k_m})^4. \tag{8}$$

Consider the closed-loop transfer function $G_c(s)$ between r and y_p,

$$G_c(s) = \frac{c_0 k_p N_p \Lambda^2}{\Lambda \left[(\Lambda - \theta_1^T \alpha(s)) D_p - k_p N_p (\theta_2^T \alpha(s) + \theta_3 \Lambda) \right]}. \tag{9}$$

By choosing $c_0 = \frac{k_m}{k_p}$, finding adequate values for $\theta_1, \theta_2, \theta_3$ and by our previous selection of $\Lambda(s)$, the zeros of the plant, $N_p(s)$, are canceled, and replaced by those of the reference model, $N_m(s)$, so that $G_c(s) = W_m(s)$.

3.3 Adaptive Law

In this section, we present an adaptive mechanism that adjusts continuously the vector of controller parameters, $\theta = \left[\theta_1^T, \theta_2^T, \theta_3, c_0\right]^T$, so that a parameterized model (whose structure is the same as that of the plant model) approaches the model reference as t increases.

Consider the parametric model,

$$z = W_m u_p = \theta^{*T} \phi_p, \tag{10}$$

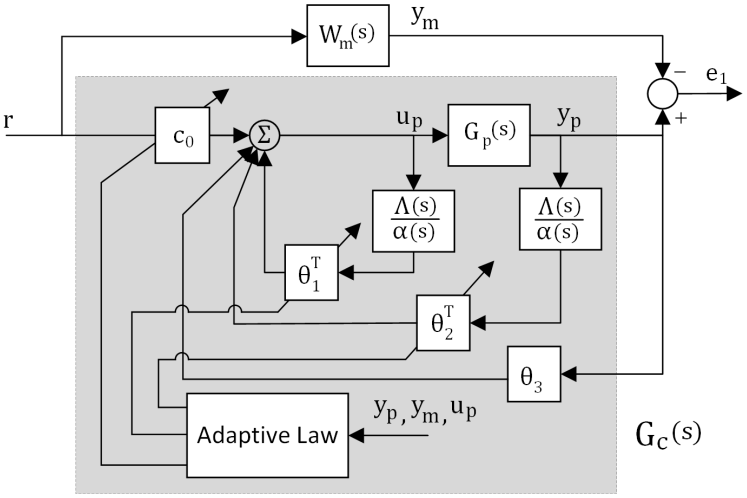

Figure 5. Structure of the MRAC scheme. Eq. (7)
(Ioannou and Sun, 2013)

where θ^{*T} is the vector of optimal values for θ, ϕ_p is vector containing the plant I/O signals of G_p expressed in terms of the reference model, W_m:

$$\phi_p = \left[W_m(s)\frac{\alpha(s)^T}{\Lambda(s)}u_p, \quad W_m(s)\frac{\alpha(s)^T}{\Lambda(s)}F_s, \quad W_m(s)F_s, \quad F_s \right]^T. \tag{11}$$

Finally, we use an adaptive law based on least-squares to estimate θ, by

$$\dot{\theta} = P\epsilon\phi_p \tag{12}$$

$$\dot{P} = -P\frac{\phi_p\phi_p^T}{m^2}P, \quad \text{with } P(0) = P^T(0) > 0$$

$$\epsilon = \frac{z-\hat{z}}{m^2} = \frac{W_m u_p - \theta^T\phi_p}{m^2}, \tag{13}$$

where P is a $_{n\times n}$ matrix called the covariance matrix, ϵ is the normalized estimation error, $\hat{z}$ is the estimated output of the parametric model, and m is a normalizing signal chosen as $m^2 = 1 + \phi_p^T\phi_p$.

4. RESULTS

In order to perform a preliminary validation of the proposed control scheme, we first developed a simulator of the SRPAR-Human system using the SimMechanics toolbox of Simulink-MATLAB. Then, we performed a set of simulations using the force and impedance controllers proposed in the previous section.

4.1 Force control response

Figure 6 shows the temporal response of the force control tracking the reference signal ($F_s^d = 100\sin(2\pi * f * t)$) where $f = 1$ Hz. We performed simulations for four different conditions, a first condition when the platform is mechanically fixed (1-blue), and for three different combinations of parameters of the human impedance: (2-red) human resistive or high-impedance, (4-magenta) human passive or low-impedance, and (3-yellow) an intermediate human impedance. Simulations where performed using the values from Table 2. We observed a good performance of the simulated response, and how the adaptation law allowed the improvement of such performance, as highlighted in the zoom boxes.

Table 2. Human Parameters

Parameter	Mode2	Mode3	Mode4
J_h (kg· m^2)	0.1	0.05	0.03
C_h (N·m·s/rad)	9	7	5
K_h (N·m/rad)	100	50	20

Figure 6b presents the force error, $F_e = F_s^d - F_s$, which converged in the cases 2, 3 and 4 toward the error of the case 1. This was expected since the case 1 corresponds to the model reference $W_m(s)$. Figure 6c shows the control

signal, u_p, given by the motor angular velocity. Notice that the lower the plant impedance the greater the magnitude of the control signal. This is an important aspect that reflects how the adaptive control compensates the difference between the reference model and the actual plant. Thus, the control signal is higher as lower the human impedance. Figure 6d presents the temporal evolution of the estimation error, $\epsilon = z - \hat{z}$, for all operation modes. Since ϵ diminishing along time, we interpret that the control parameters, θ_c, are converging to values that improve the model estimation and leading to a better control performance.

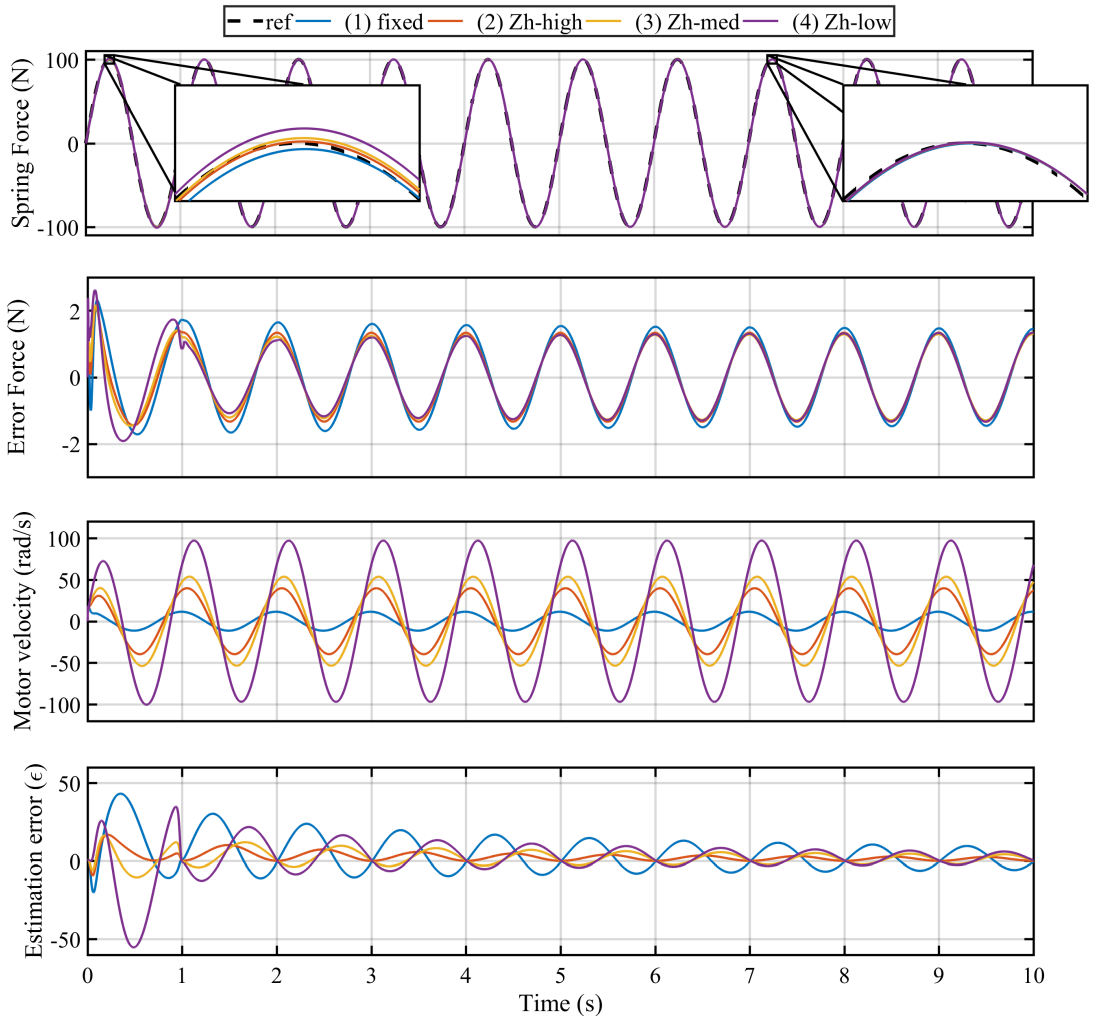

Figure 6. Sine response of the proposed force controller

Figure 7 shows the response of the system to a step signal. Notice how the controller ensures stability and zero steady-state error for all cases. However, the response presents a large peak in the control signal, which is limited by a saturation block similar to the present in the real platform. Despite this limitation, the rise time is considerably low.

We also compared the response of the proposed control, i.e. $\mathcal{H}_\infty$+ MRAC, with the response of the $\mathcal{H}_\infty$ controller alone. To do that, we simulated both controllers for the four above mentioned cases. Figure 8 presents the comparison between the temporal responses of both controllers. From the graphs, the proposed scheme reduces the force tracking error with respect to the non-adaptive configuration. The graphs also highlight the fact that a fixed-gain controller can not guarantee the same performance for the different conditions during the system operation as result of variations of the human impedance (Perez-Ibarra *et al.*, 2017). An important aspect observed was that our proposed scheme does not require a significant high control signal, as can be observed at Figure 8c.

4.2 Impedance control response

In order to evaluate the stability and performance of the proposed force controller during impedance controlled operation of the platform, we simulated the impedance control tracking a kinematic reference. We performed simulations for the four cases described in the previous section. We defined $K_v = 50$ N·m and $B_v = 1$ N·m·s in (5).

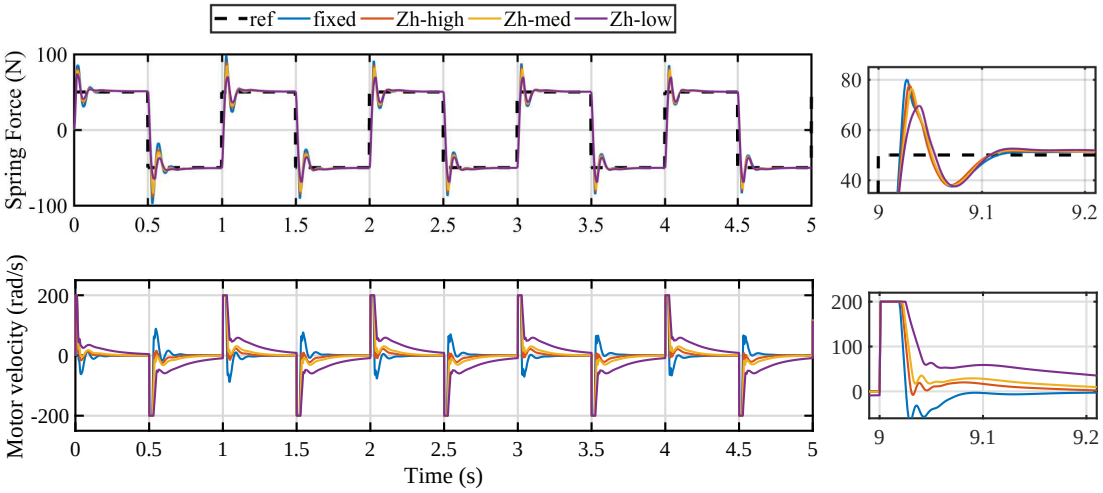

Figure 7. Step Response of the Proposed Force Controller

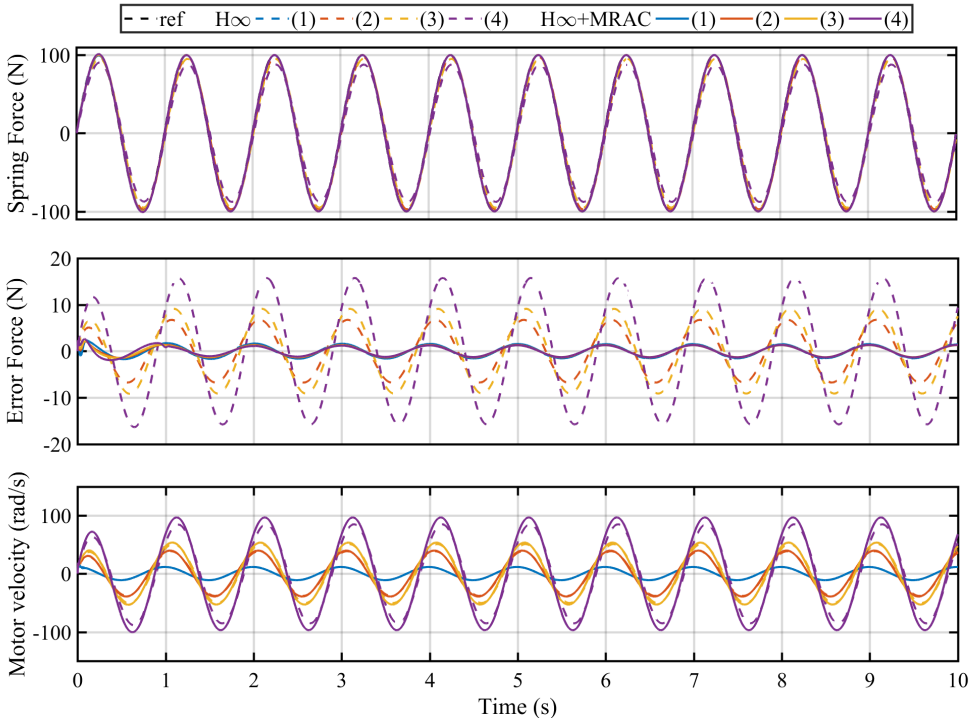

Figure 8. Comparison of responses of the $\mathcal{H}_\infty$ and $\mathcal{H}_\infty$+MRAC controllers

Figure 9 shows the impedance and force control responses. As expected, the tracking of the position is better as lower is the human impedance. Figure 9b shows the platform torque, τ_r, which as expected is higher in the fixed case as the position error is higher in this case. In addition, Figure 9c shows that the main control signal of the system, i.e. the angular velocity of the motor w_m, is bounded and coherent with the results of the previous section.

5. CONCLUSIONS

We proposed a force-impedance control strategy based on $\mathcal{H}_\infty$ and MRAC that showed stability and high performance for a system with partially unknown parameters. We performed a set of simulations of the SRPAR dynamics for four different conditions of operation of the platform: mechanically-fixed and three different ankle joint impedances. For all the conditions the adaptive scheme improved the force tracking performance by compensating the differences between the reference model and the actual plant. This research is a starting point for future implementation in the SRPAR and others rehabilitation robotic systems which using SEA's.

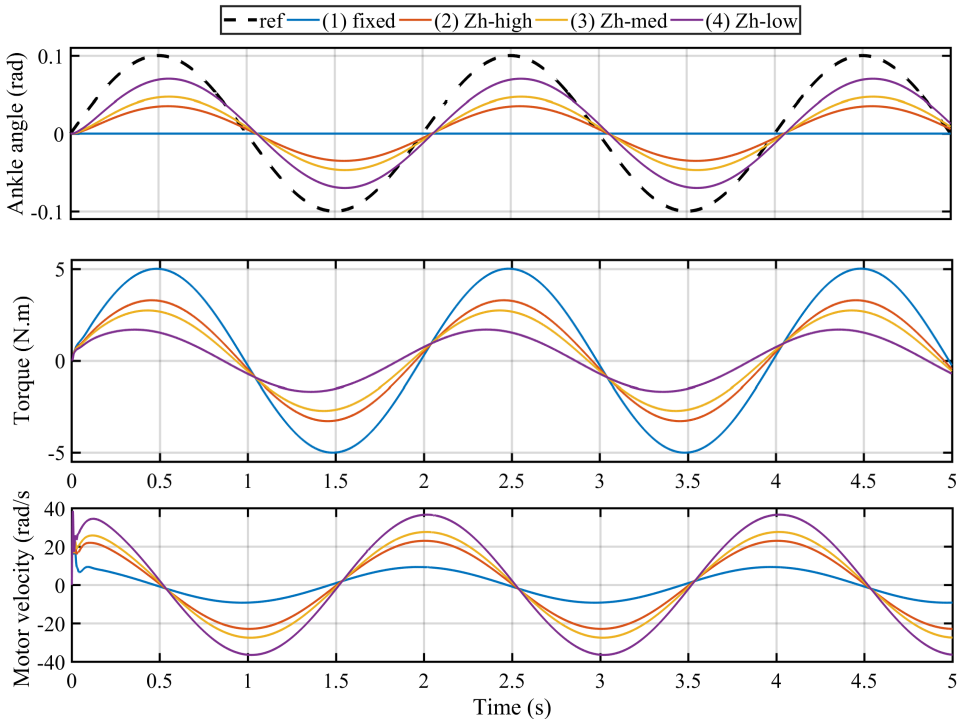

Figure 9. Impedance control response using the $\mathcal{H}_\infty$+MRAC control squeme

6. REFERENCES

Calanca, A. and Fiorini, P., 2014. "Human-adaptive control of series elastic actuators". *Robotica*, Vol. 32, No. 8, pp. 1301–1316.

Chang, W.H. and Kim, Y.H., 2013. "Robot-assisted therapy in stroke rehabilitation". *Journal of stroke*, Vol. 15, No. 3, p. 174.

Goncalves, A.C.B.F., dos Santos, W.M., Consoni, L.J. and Siqueira, A.A.G., 2014. "Serious games for assessment and rehabilitation of ankle movements". In *Serious Games and Applications for Health (SeGAH), 2014 IEEE 3rd International Conference on*. pp. 1–6.

Hogan, N., 1985. "Impedance control: an approach to manipulation". *Journal of Dynamic Systems, Measurement and Control*, Vol. 107 (Parts 1-3), No. 1, pp. 1–24.

Hussain, S., Xie, S.Q. and Jamwal, P.K., 2013. "Adaptive impedance control of a robotic orthosis for gait rehabilitation". *IEEE Transactions on Cybernetics*, Vol. 43, No. 3, pp. 1025–1034. ISSN 2168-2267. doi: 10.1109/TSMCB.2012.2222374.

Ioannou, P. and Sun, J., 2013. *Robust Adaptive Control*. Dover Publications. ISBN 9780486320724.

Jutinico, A.L., Jaimes, J.C., Escalante, F.M., Perez-Ibarra, J.C., Terra, M.H. and Siqueira, A.A.G., 2017a. "Recursive robust regulator for discrete-time markovian jump linear systems: Control of series elastic actuators". In *20th IFAC World Congress*.

Jutinico, A.L., Jaimes, J.C., Escalante, F.M., Perez-Ibarra, J.C., Terra, M.H. and Siqueira, A.A.G., 2017b. "Impedance control for robotic rehabilitation: A robust markovian approach". *Frontiers in Neurorobotics*, Vol. 11, p. 43. ISSN 1662-5218. doi:10.3389/fnbot.2017.00043. URL `https://www.frontiersin.org/article/10.3389/fnbot.2017.00043`.

Lopez, R., Aguilar, H., Salazar, S. and Lozano, R., 2014. "Adaptive control for passive kinesiotherapy elltio". *Journal of Bionic Engineering*, Vol. 11, No. 4, pp. 581 – 588. ISSN 1672-6529. doi:https://doi.org/10.1016/S1672-6529(14)60069-X.

Maciejasz, P., Eschweiler, J., Gerlach-Hahn, K., Jansen-Troy, A. and Leonhardt, S., 2014. "A survey on robotic devices for upper limb rehabilitation". *Journal of neuroengineering and rehabilitation*, Vol. 11, No. 1, p. 3.

Perez-Ibarra, J.C., Jutinico, A.L., Jaimes, J.C., Ortega, F.M.E., Terra, M.H. and Siqueira, A.A.G., 2017. "Design and analysis of $\mathcal{H}_\infty$ force control of a series elastic actuator for impedance control of an ankle rehabilitation robotic platform". In *2017 American Control Conference (ACC)*. pp. 2423–2428. doi:10.23919/ACC.2017.7963316.

Pratt, G.A. and Williamson, M.M., 1995. "Series elastic actuators". In *Proceedings 1995 IEEE/RSJ International Confer-*

ence on Intelligent Robots and Systems. Human Robot Interaction and Cooperative Robots. Vol. 1, pp. 399–406 vol.1. doi:10.1109/IROS.1995.525827.

Sharifi, M., Behzadipour, S. and Vossoughi, G., 2014. "Model reference adaptive impedance control in cartesian coordinates for physical human-robot interaction". *Advanced Robotics*, Vol. 28, No. 19, pp. 1277–1290. doi: 10.1080/01691864.2014.933125.

Wolbrecht, E.T., Chan, V., Reinkensmeyer, D.J. and Bobrow, J.E., 2008. "Optimizing compliant, model-based robotic assistance to promote neurorehabilitation". *IEEE Transactions on Neural Systems and Rehabilitation Engineering*, Vol. 16, No. 3, pp. 286–297. ISSN 1534-4320. doi:10.1109/TNSRE.2008.918389.

7. RESPONSIBILITY NOTICE

The authors are the only responsible for the printed material included in this paper.